



Original article

An effort to discover the preferred conformation of the potent AMG3 cannabinoid analog when reaching the active sites of the cannabinoid receptors

Serdar Durdagi^{a,*}, Manthos G. Papadopoulos^b, Thomas Mavromoustakos^{c,**}^aInstitute for Biocomplexity and Informatics, Department of Biological Sciences, University of Calgary, Calgary, Alberta, Canada^bInstitute of Organic and Pharmaceutical Chemistry, The National Hellenic Research Foundation, Athens, Greece^cDepartment of Chemistry, University of Athens, Athens, Greece

ARTICLE INFO

Article history:

Received 13 May 2011

Received in revised form

29 August 2011

Accepted 6 October 2011

Available online 15 October 2011

Keywords:

Cannabinoids

3D-QSAR

MD simulations

Molecular Docking

De novo drug design

CB1 and CB2 receptors

ABSTRACT

Most of current 3D-QSAR algorithms use alignments of compounds at the training set based on reference active ligands in the first step of the construction of the pharmacophore modeling. This first step mostly defines the success of constructed pharmacophore models. In this step, it is essential to find the bioactive conformation for solid and reliable 3D-QSAR models. Therefore, we have proceeded through different approaches for revealing the preferred conformations of Δ^8 -THC derivative AMG-3 at CB1 and CB2 receptors. In the first approach, we have applied conformational search methods in gas and in solvent phases for the ligand. The derived low energy conformers using these methodologies have been modeled through 3D-QSAR studies (first generation model). In the second approach, the low energy conformers derived from molecular docking studies have been used as input for 3D-QSAR studies (second generation model). In the current study, a new approach using MD calculations in a simulated biological environment, thus the CB receptors surrounded by a lipid bilayer environment has been used (third generation). The obtained results for different environments were compared and the approach deriving the highest statistic results was used for the generation of the novel AMG3 analogs for optimal and selective binding affinities at CB1 and CB2 receptors by the *de novo* drug design modeling.

© 2011 Elsevier Masson SAS. All rights reserved.

1. Introduction

Most of current 3D quantitative structure–activity relationships (3D-QSAR) algorithms use alignments of compounds at the training set based on conformations of reference ligands (i.e. high affinity template ligands from the training set) at the first step of the construction of the pharmacophore modeling. This step mostly defines the success of constructed pharmacophore models. Thus, in this step, it is essential to find the correct conformation of the reference molecule that adopts when it fits its target binding site. In drug design, the receptor-bound conformation of ligand, which is called “bioactive conformation”, is especially important. However, a flexible molecule with several rotatable bonds can adopt many conformations. AMG3 [(6aR,10aR)-3-(2-hexyl-1,3-dithiolan-2-yl)-6,6,9-trimethyl-6a,7,10,10a-tetrahydrobenzo[*c*]chromen-1-ol] (Fig. 1) is a derivative of Δ^8 -THC possessing a flexible chain and a dithiolane group [1]. Since AMG3 is a potent agonist with sedative and

analgesic effects and showing high binding affinity at both CB1 and CB2 receptors (K_i of 0.32 nM and 0.52 nM, correspondingly) we have used it as a template for structural development of novel cannabinoid (CB) drugs [2–7].

The question we set to answer is “which is the preferred conformation” that adopts a molecule during the interaction with the active site amino acid residues of the receptor? The question sounds pretty difficult to be answered and indeed it is. QSAR studies on low energy conformers derived through geometry optimizations or subjected to systematic conformational search analysis can be used. However, the model to be built is not necessarily the optimum because these low energy conformers may not represent the real ones. We have worked out this approach in our previous studies and called the derived statistical model from QSAR studies “first generation” model [6,36].

The second approach is to use the low energy conformers at QSAR studies derived from molecular docking. Docking studies provide poses of the drug at the active site of the receptor but usually they do not account of the flexibility of the receptor's side chains or its environment. We called the derived model as second generation and statistical results derived from this approach has been improved in respect to the first generation model [4,6].

* Corresponding author.

** Corresponding author.

E-mail addresses: durdagis@ucalgary.ca (S. Durdagi), tmavrom@chem.uoa.gr (T. Mavromoustakos).

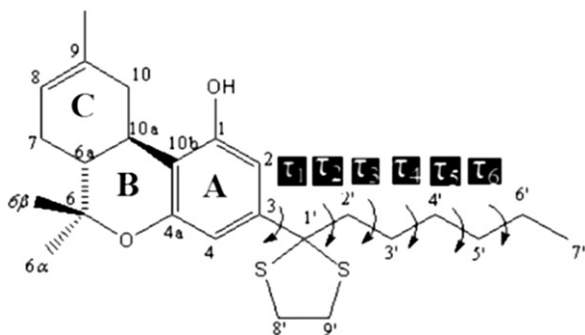


Fig. 1. Molecular structure of AMG3. (τ_1 , C2–C3–C1'–C2'; τ_2 , C3–C1'–C2'–C3'; τ_3 , C1'–C2'–C3'–C4'; τ_4 , C2'–C3'–C4'–C5'; τ_5 , C3'–C4'–C5'–C6'; τ_6 , C4'–C5'–C6'–C7').

In current research work, molecular dynamics (MD) simulations were performed for the drug at the binding site of the receptor environment surrounded by a lipid bilayer. Derived low energy conformations from MD simulations were used in QSAR studies. This environment is simulating more closely the biological medium as it is assumed that incorporation of lipophilic ligands such as the CBs are first embedded into the plane of membranes containing the CB receptors that facilitate their approach to the binding site of the receptor through lateral diffusion [8–10]. A similar diffusion-controlled mechanism of receptor approach was also proposed for binding between amphipathic neuropeptides and G-protein coupled receptors (GPCRs), as well as the widely used synthetic CB ligand, CP-55,940 [11–18]. Thus, it is pointed out that the ligand needs to approach the receptor at a particular depth in the lipid matrix and in particular orientation(s) to be able to reach the binding pocket efficiently. Obtained QSAR results were analyzed and *de novo* drug design studies were performed in order to derive AMG3 analogs for optimal and selective binding affinities at CB1 and CB2 receptors.

2. Methods

2.1. Geometry optimizations of investigated systems

The structures of studied molecules [36] were subjected to geometry optimizations using a combination of Powell energy minimization algorithm, Gasteiger–Huckel charges and 0.001 kcal/mol Å energy gradient convergence criterion using the standard Tripos MM force field of the Sybyl molecular modeling package [19]. For the conformational analysis of template compound used in 3D-QSAR, *ab initio* B3LYP/6-31G* level QM calculations were also performed.

2.2. Monte Carlo (MC) simulations

MC analysis of ligands has been carried out with the CHARMM force field of QUANTA package [20] as well as the semi-empirical methods of AM1 and PM3 (SCF convergence criterion has been set to 10^{-6} as energy gradient convergence limit).

2.3. 3D-QSAR settings

The comparative molecular similarity indices (CoMSIA) 3D-QSAR algorithm was used [21]. The steric and electrostatic field energies were calculated using the Lennard–Jones and the Coulomb potentials, respectively with a $1/r$ distance-dependent dielectric constant in all intersections of a regularly spaced (2 Å) grid. An sp^3 carbon atom with a radius of 1.53 Å and a charge of +1.0 was used as a probe to calculate the steric and electrostatic energies between the probe and the molecules using the Tripos force field. The truncation for both the steric and electrostatic energies was set to 30 kcal/mol. The initial partial least square (PLS) analysis was performed using the “leave-one-out” cross-validation method for all 3D-QSAR analyses. A minimum column filtering value of

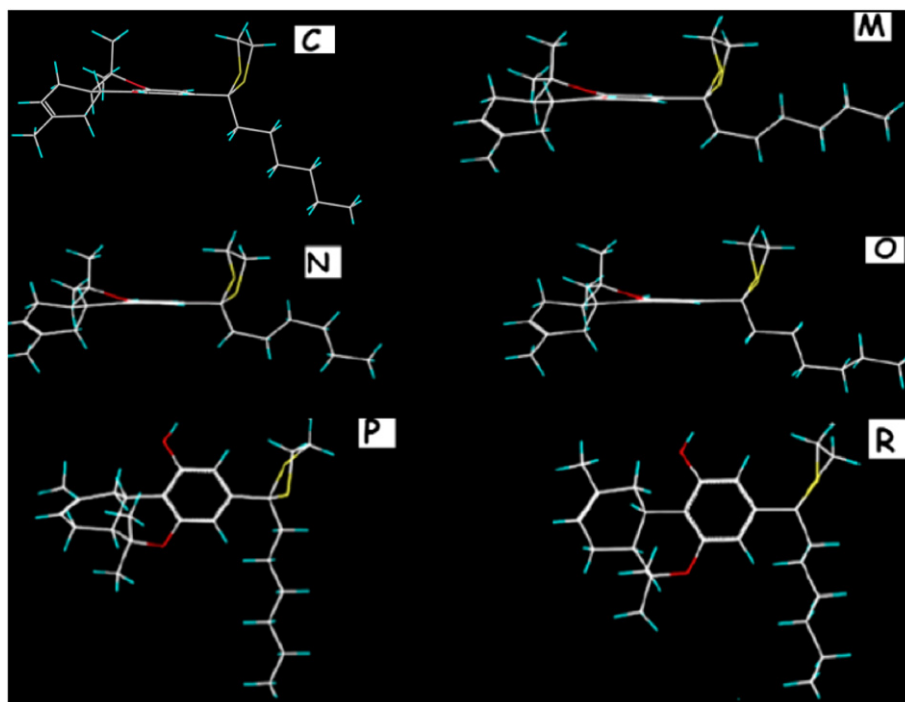


Fig. 2. MD simulations of AMG3 at the active site of the receptors produced **C**, **M**, **N**, **O**, **P** and **R** conformers. At the active site of the CB1 receptor, conformers **C**, **M**, **N** and **O**; at the active site of the CB2 receptor, conformers **P** and **R** are found as favored conformations of AMG3. At the alkyl side chain these conformers have following dihedral angles τ_1 – τ_6 : **C** (*gauche*+/*gauche*+/*trans*/*trans*/*trans*/*trans*); **M** (*gauche*+/*trans*/*gauche*+/*trans*/*trans*/*trans*); **N** (*gauche*+/*trans*/*gauche*+/*trans*/*gauche*-/*trans*); **O** (*gauche*+/*trans*/*trans*/*trans*/*gauche*-/*trans*); **P** (*trans*/*gauche*-/*trans*/*trans*/*trans*/*trans*) and **R** (*trans*/*gauche*-/*trans*/*gauche*-/*trans*/*trans*).

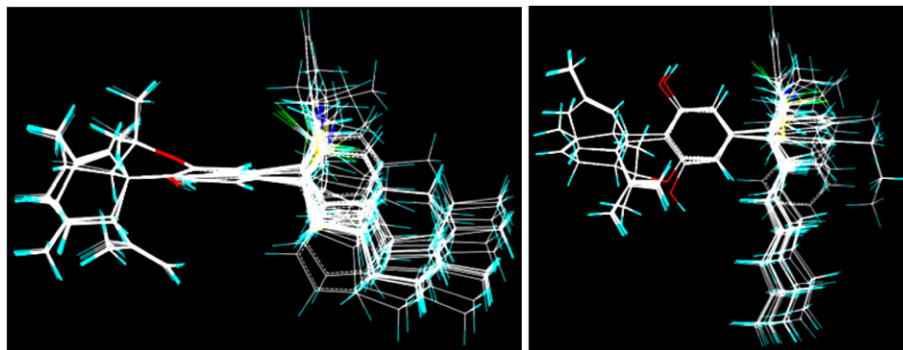


Fig. 3. Structural alignments of the compounds in the training set for constructing 3D-QSAR/CoMSIA models based on template ligand AMG3. Superimposition was performed based on conformer **O** for CB1 model (on the left); and conformer **P** for CB2 model (on the right).

2.00 kcal/mol was set to improve the signal to noise ratio by omitting those grid points whose energy variation was below this threshold. In both CoMFA and CoMSIA analyses, the descriptors were treated as independent variables, whereas the pK_i values were treated as dependent variables in the PLS regression analyses in order to derive the 3D-QSAR models. The final model (non-cross-validated conventional analysis) was developed from the model with the highest r_{cv}^2 , and the optimum number of components was set equal to that yielding the highest r_{cv}^2 . The non-cross-validated models were assessed by the conventional correlation coefficient r^2 , standard error of prediction, and F values. For the creation of the CoMFA field, 'CoMFA standard' scaling was selected, while in the case of CoMSIA 'none' option was selected in the Sybyl.

2.4. Molecular docking

Flexible docking studies have been applied using FlexX program [22] of Sybyl molecular modeling package [19]. FlexX is a flexible docking method that uses an incremental construction algorithm to place ligands into a binding site of a receptor. The base fragment (the ligand core) is automatically selected and placed into the active site of the receptor using a pose clustering algorithm. Then, the remainder of the ligand is built up incrementally from other fragments. Subsequently, placement of the ligand is scored on the basis of protein–ligand interactions and the binding energy is estimated and placements are ranked. Finally, the obtained placements are ranked. 3D models of the CB1 and CB2 receptors based on template rhodopsin from Tuccinardi et al. [23] have been used for the initial

docking experiments, however, the critical binding site residues were determined from several molecular modeling studies of CB receptors (e.g., Tuccinardi et al. [23], Salo et al. [24] and Shim et al. [25]). The active site in the docking runs included all atoms within a radius of 6.5 Å around the critical amino acids for CB1 receptor: Phe174, Leu190, Lys192, Leu193, Gly195, Val196, Thr197, Phe200, Thr201, Pro251, Trp356, Leu359, Ser383, Cys386, Leu387 and for CB2 receptor: Leu108, Ser112, Pro168, Leu169, Trp194, Trp258.

2.5. MD simulations

The MD simulations were performed with Groningen Machine for Chemical Simulations (GROMACS) version 3.3.1 software package [26] using the gmx force field. Simulations were run with periodic boundary conditions. The coordinates of AMG3-conformers were used as input at the PRODRG program [27] in order to obtain topologies which will be used in the MD simulations. DPPC lipid bilayer for the MD simulations was obtained from Dr. M. Karttunen (128 DPPC lipids and 3655 water molecules after 100 ns) [28]. Simulations were run in the NPT ensemble at 300 K and 1 bar with periodic boundary conditions. Berendsen barostat and thermostat algorithms were used [29]. Electrostatic interactions were calculated using the particle mesh Ewald method [30]. Cut-off distances for the calculation of Coulomb and van der Waals interactions were 1.0 and 1.4 nm, respectively. Prior to the dynamics simulation, energy minimization calculations were applied to the full system without constraints using the SD method for 5000 steps with the initial step size of 0.01 Å (the minimization

Table 1
Derived statistical results of third generation (based on template conformation derived from MD simulations of template molecule at the membrane-associated CB1 and CB2 receptors) of CB1 and CB2 models. (For easier comparison, results of first and second generation of models were also included in the Table. First generation of models was based on favored template conformation in solution, and second generation of the models was based on docking results, reported previously [4,36]).

	CB1 model-first generation (template ligand AMG3-conformer A)	CB1 model second generation (template ligand AMG3-conformer C)	CB1 model third generation (template ligand AMG3-conformer O)	CB2 model-first generation (template ligand AMG3-conformer A)	CB2 model second generation (template ligand AMG3-conformer C)	CB2 model third generation (template ligand AMG3-conformer P)
Number of compounds in the training set	30	30	30	29	29	29
r_{cv}^2	0.746	0.764	0.771	0.625	0.645	0.710
r^2	0.944	0.953	0.962	0.912	0.940	0.952
Standard error of estimate (SEE)	0.296	0.272	0.244	0.324	0.247	0.246
F	65.031	77.600	97.623	47.855	57.491	72.373
Relative contributions of steric:electrostatic fields	0.890:0.110	0.890:0.110	0.852:0.148	0.918:0.082	0.885:0.115	0.853:0.147
Number of optimal components	6	6	6	5	5	5

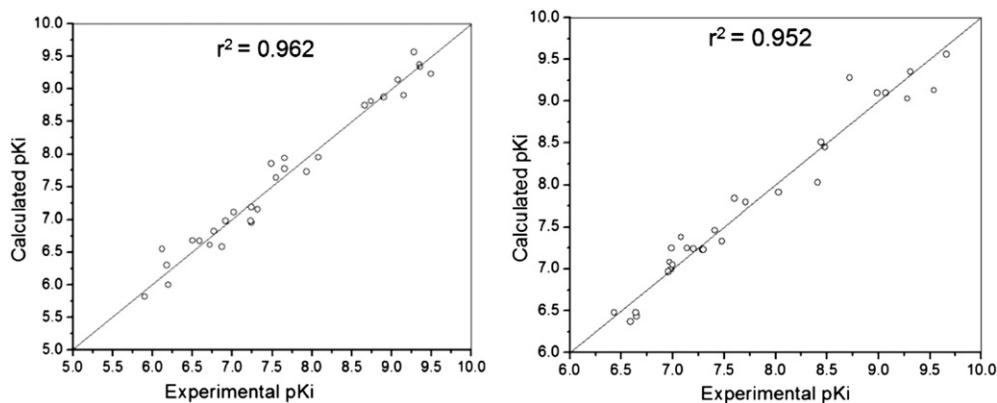


Fig. 4. Plots of experimental and predicted values of binding affinities (given as pK_i) of CB analogs in the training set obtained by third generation of 3D-QSAR (left) CB1 model and (right) CB2 model.

tolerance was set to 100 kJ/(mol nm)). The system was then equilibrated via 250 ps simulations with a time step of 2 fs, subsequently a 2.5 ns simulations were performed at 300 K and 1 bar with a time step of 2 fs. All bonds were constrained using the LINCS algorithm [31]. Stability of MD simulation is tested by potential energy change during the simulations and receptor backbone RMSD versus time plots throughout the MD simulations (see Fig. S1). The studies are performed to the average structure derived from last 0.5 ns simulations of the trajectories.

2.6. LeapFrog *de novo* drug design studies

LeapFrog algorithm under Sybyl [19] is used in order to automatically generate a series of ligands for the binding pocket of a receptor. LeapFrog is a second generation *de novo* drug discovery program for the design of potentially active compounds using molecular evolution or electronic screening, by repeatedly making structural changes and then either keeping or discarding the obtained results, depending on the binding energy results. There are two starting input options in order to generate site point probe

atoms that will be used in the binding energy calculations, these are a pharmacophore model or a receptor structure. The charge of the site point probe atom is positive, negative or lipophilic and its value is compared with ± 1.0 : if the value is smaller than $+1.0$, it is lipophilic, if the value is bigger than $+1.0$, site points seek a negatively charged atom and if the value is less than -1.0 , site points seek a positively charged atom in the fragment. Template compound AMG3 was selected as starting structure. Firstly, the OPTIMIZE module was used for the improvement in binding energy. Secondly, several moves such as JOIN, FUSE, BRIDGE and OPTIMIZE options were used after the initial run of 100 moves taken into account the synthetic difficulties. The derived ligands that had the best binding energy were used for repeating the cycle of 5000 moves.

3. Results and discussion

3.1. Building of the “third generation” of 3D-QSAR models and comparison with previously reported “first” and “second” generations

Alignment is the most difficult part in the contemporary drug design since it contains the not well-resolved yet problem of conformational search [32]. Therefore, conformational search of the reference ligands must be worked thoroughly. For this aim, we performed extensive conformational search analysis for the CB ligands [6,7]. In the current study, we performed MD simulations of AMG3 ligand at the binding site of the receptor which is merged with lipid bilayer.

Torsional angle screening results of MD analysis showed that conformers **C**, **M**, **N** and **O** of AMG3 favor at the active site of the CB1,

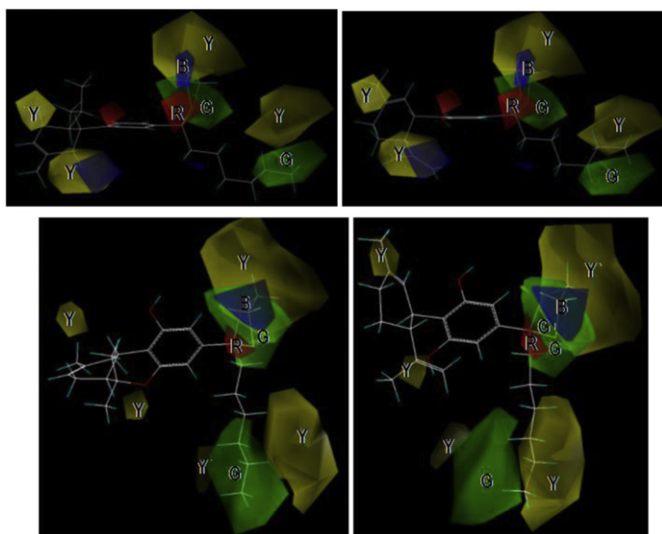


Fig. 5. Steric and electrostatic contour maps of AMG3 (on the left, top) and its corresponding cannabidiol (CBD) analog **13** (on the right, top) for the CB1 receptor using the template ligand as conformer **O**; and corresponding steric and electrostatic contour maps (compounds AMG3 (on the left, bottom) and **13** (on the right, bottom)) for the CB2 receptor using the template ligand as conformer **P**.

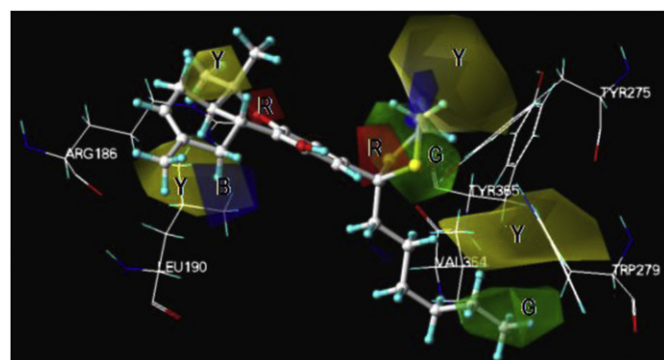


Fig. 6. Contour plots derived from third generation of QSAR of CB1 model merged with CB1 atomistic receptor model.

Table 2
The proposed novel CB analogs by *de novo* drug design program LeapFrog based on CB1 model and their predicted pK_i values for CB1 receptor.

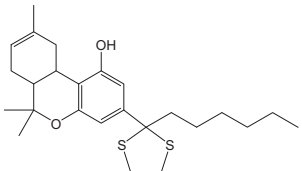
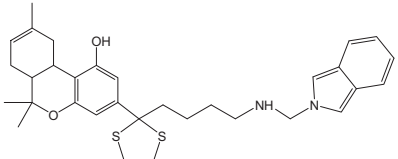
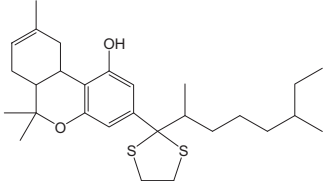
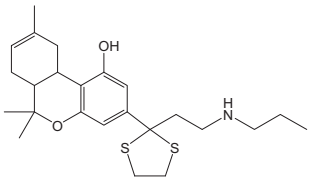
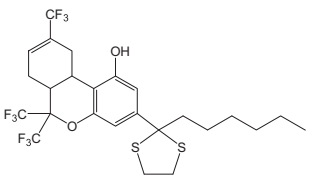
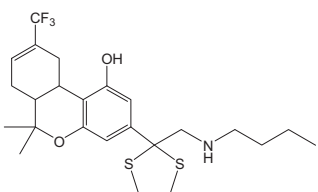
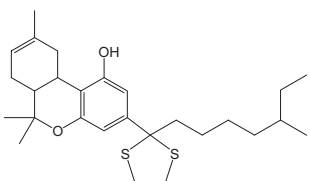
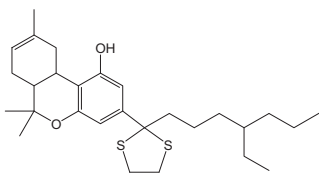
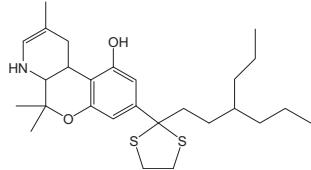
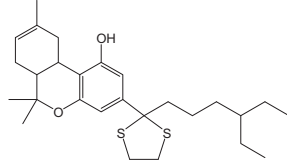
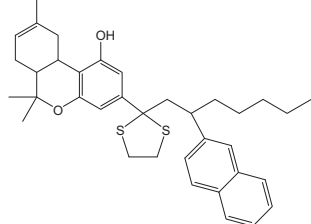
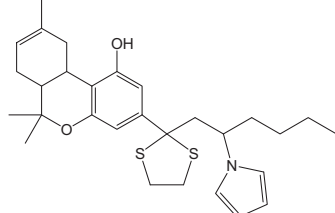
Compound	Structure	CB1 model predicted pK_i
Ref		9.23
D1		9.73
D2		9.43
D3		9.39
D4		9.35
D5		9.32
D6		9.32
D7		9.31

Table 2 (continued)

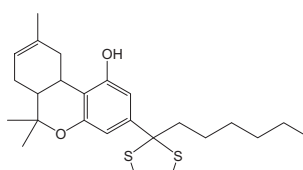
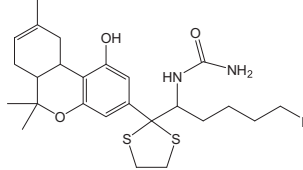
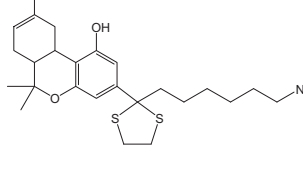
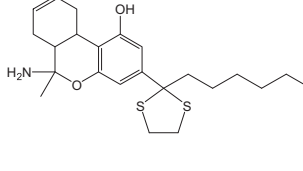
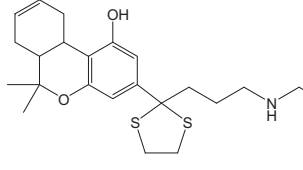
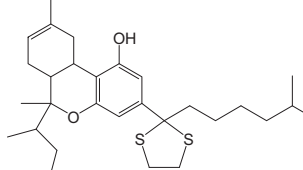
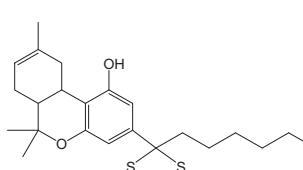
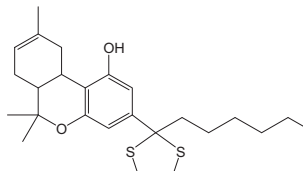
Compound	Structure	CB1 model predicted pK_i
D8		9.28
D9		9.28
D10		9.27
D11		9.24

and conformers **P** and **R** favor at the binding site of the CB2 receptor (Fig. 2). The letters used are to avoid confusion with other letters of “first” and “second” generation models reported [6,7]. Structures of the Δ^8 -THC analogs and their measured activities at CB1 and CB2 receptors were used for the third generation of CB1 and CB2 models (see Supporting Material, Table S1). Initial statistical tests for the derived models showed optimal statistical results using template conformer **O** for the CB1 and conformer **P** for the CB2 models. Therefore, further analysis is performed using these template conformers. Fig. 3 shows the superimpositions of CB analogs used as a training set to construct 3D-QSAR/CoMSIA models based on the conformers **O** and **P** of template ligand. Table 1 shows the derived statistical results for CB1 and CB2 models including those of first and second generation of models (i.e. low energy conformations of template ligand in solution and at the binding site of receptor based on docking simulations, respectively) for direct comparison. In this table, some statistical results such as r^2 , SEE, r_{cv}^2 and F for each model were used to evaluate the training set and test set predictions. Analysis of these results (i.e. highest r^2 , r_{cv}^2 and lowest SEE values for third generation of both CB1 and CB2 models) clearly show that the using template conformer derived from MD simulations of ligand at the binding site of the receptor merged with lipid bilayers improves statistical results, significantly.

Experimental and corresponding predicted affinities of CB analogs were plotted at Fig. 4. Fig. 5 shows the steric and electrostatic contour maps of AMG3 (on the left, top) and its corresponding CBD analog **13** (on the right, top, see Supporting Information, Table S1) for the CB1 receptor using the conformer **O** as template ligand. The

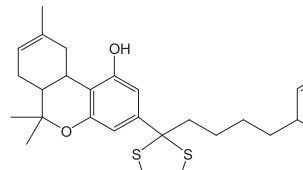
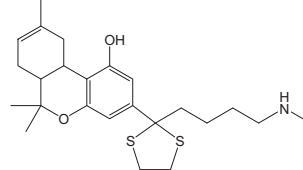
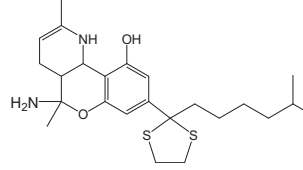
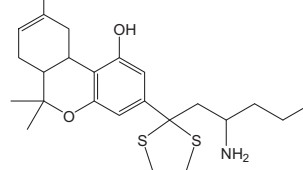
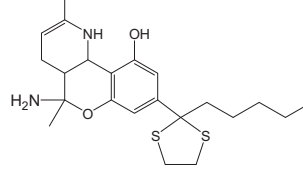
Table 3

The proposed novel CB analogs by *de novo* drug design program LeapFrog based on CB2 model and their predicted pK_i values for CB2 receptor.

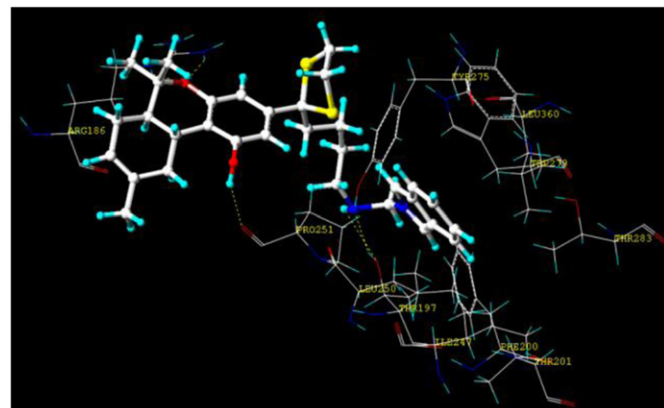
Compound	Structure	CB2 model predicted pK_i
Ref.		9.03
D12		9.52
D13		9.42
D14		9.40
D15		9.39
D16		9.36
D17		9.34
D18		9.33

(continued on next page)

Table 3 (continued)

Compound	Structure	CB2 model predicted pK_i
D19		9.26
D20		9.26
D21		9.25
D22		9.23
D23		9.15

corresponding steric and electrostatic contour maps for AMG3 and CBD analog **13** for the CB2 receptor using conformer **P** as the template ligand are also shown in the Fig. 5 (bottom). Green and yellow colored contour maps show sterically favorable and

**Fig. 7.** Binding interactions of **D1** at the binding site of the CB1 receptor.

unfavorable regions, respectively. Blue and red colored contour plots show electropositive and electronegative regions, respectively. Although similar contour plots with initially generated models (first and second generations [6,7]) were derived from the third generation; careful analysis of contour plots have shown some fine and critical differences for the third models. For example, the orientation of alkyl chain of AMG3 is more restricted in the CB2 models, since left and right sides of the tail of the alkyl chain include yellow colored sterically unfavorable contours, and between these contours there is a green colored sterically favorable contour (Fig. 5, bottom [For interpretation of the references to color in this figure, the reader is referred to the web version of this article.]). Derived contour plots from third generation of QSAR models have merged with the receptor coordinate files (Fig. 6). Results confirmed the accuracy of derived contour plots. For example, sterically unfavorable contours of CB1 model fit with the side chains of the amino acid residues at the binding site of the CB1 receptor (e.g., Leu190, Arg186, Trp279, Tyr275, Tyr355 and Val364) (Fig. 6).

3.2. De novo drug design studies of CB analogs

The optimal derived PLS analyses of CB analogs, which are produced from third generation of QSAR models, were used to generate each site points for CB1 and CB2 models. These site points were used in the *de novo* drug discovery program LeapFrog, for the predictions of novel hits by repeatedly making structural changes and then either keeping or discarding the results. Since third generation of CB1 and CB2 models were derived based on different conformations of template conformers, a selectivity of new generated ligand structures by LeapFrog can be expected. The new ligand structures were evaluated based on their binding energies, and structures that have better binding energy than reference compound (template compound, AMG3) were collected. Tables 2 and 3 show these structures for CB1 and CB2 receptors, respectively. Predicted binding affinities based on derived QSAR models were also included in the tables. Derived *de novo* designed ligands show some micro-modifications on template ligand AMG3. Thus, no difficulty is expected for their synthesis. Furthermore, synthesis of similar drugs by S. Nikas et al. [34] shows synthetic feasibility of these ligands. Derived molecules that have highest predicted binding affinity for CB1 and CB2 receptors (**D1** and **D12**, respectively) were docked at the binding site of the CB1 and CB2 receptors, respectively (Figs. 7 and 8). Their predicted high binding

affinities confirmed by better docking scores than AMG3 (i.e., **D1** and **D12** have binding scores of -19.11 kJ/mol and -19.23 kJ/mol, respectively at CB1 and CB2 receptors compared to corresponding binding scores -11.43 kJ/mol and -12.52 kJ/mol of AMG3). The **D1** stabilizes its interactions with the binding site forming H-bonds with the amino acid residues (e.g., Arg186, Thr197 and Pro251) of the CB1 as well as van der Waals interactions with the non-polar surfaces of the active site residues of the receptor (e.g., Thr197, Phe200, Thr201, Ile247, Leu250, Pro251, Tyr275, Trp279, Thr283, Leu360). The **D12** stabilizes its interactions with the binding site forming H-bonds with the amino acid residues (e.g., Leu160, Leu163, Ser165, Tyr166, Leu167, Pro168) as well as van der Waals interactions with the non-polar surfaces of the binding site residues of the CB2 receptor (e.g., Lys109, Leu160, Leu163, Pro168, Pro187, Tyr190, Trp194, Trp258).

4. Conclusions

Our laboratory has been coupled with the investigation of conformational properties of potent CB analog AMG3 both at the active site of the receptor but also in the lipid bilayer core. It is proposed that its high activity is attributed to the fact that it is inserted into the bilayer core and then it is diffused to its active site. Our biophysical results indeed show that CB perturbs productively the lipid core at proper orientation and topography that is suitable to reach the active site of the receptor [17]. Its conformational properties have been studied *in vacuo* and solvents as well as in the active site of the receptor and have been validated with 3D-QSAR model. MD studies have been also performed in a biologically simulating environment, thus at its active site surrounded by the lipid bilayer core. We thought to apply 3D-QSAR studies in order to examine if a more reliable statistical model could be built. Indeed, the results are promising and show improvement in respect to the other previous reported *in vacuo* or solvent or active site of the receptor alone. For this reason, we have applied LeapFrog *de novo* molecular design software to generate some more structures with higher binding affinities at the CB1 and CB2 receptors.

Presently known CB analogs show susceptibility toward enzymatic hydrolysis and/or not have CB1/CB2 receptor selectivity. There is considerable interest to design CB analogs possessing selectivity, high affinity and metabolic stability [18,32,33,35]. Such analogs may supply favorable response with fewer undesirable side effects and higher metabolic stability. Since ligand based models were separately constructed for CB1 and CB2 receptor activities of ligands, derived novel analogs may show higher selectivity properties for the CB1 and CB2 receptors.

We believe that the new generated molecules can be potential for possessing high affinity and selectivity and useful for medicinal chemists who are searching for more potent CB analogs to synthesize.

Appendix. Supplementary information

Supplementary data associated with this article can be found in the online version at doi:10.1016/j.ejmech.2011.10.015.

References

- [1] T. Mavromoustakos, E. Theodoropoulou, M. Zervou, T. Kourouli, D. Papahatjis, J. Pharm. Biomed. Anal. 18 (6) (1999) 947–956.
- [2] D.P. Papahatjis, T. Kourouli, V. Abadji, A. Goutopoulos, A. Makriyannis, J. Med. Chem. 41 (7) (1998) 1195–1200.
- [3] D.P. Papahatjis, S.P. Nikas, T. Kourouli, R. Chari, W. Xu, R.G. Pertwee, A. Makriyannis, J. Med. Chem. 46 (15) (2003) 3221–3229.
- [4] S. Durdagi, M.G. Papadopoulos, D.P. Papahatjis, T. Mavromoustakos, Bioorg. Med. Chem. Lett. 17 (24) (2007) 6754–6763.

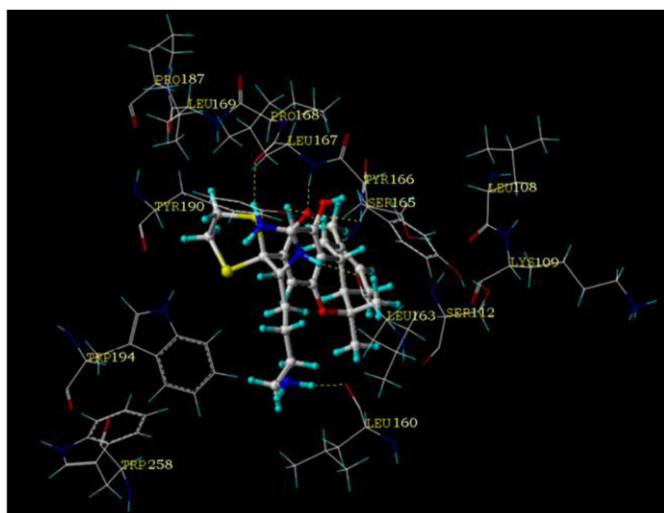


Fig. 8. Binding interactions of **D12** at the binding site of the CB2 receptor.

- [5] K. Antoniou, A. Galanopoulos, S. Vlachou, T. Kourouli, V. Nahmias, K. Thermos, G. Panagis, Z. Daifoti, M. Marselos, D. Papahatjis, C. Spyraiki, *Behav. Pharmacol.* 16 (5–6) (2005) 499–510.
- [6] S. Durdagi, H. Reis, M.G. Papadopoulos, T. Mavromoustakos, *Bioorg. Med. Chem.* 16 (2008) 7377–7387.
- [7] S. Durdagi, M.G. Papadopoulos, P. Zoumpoulakis, C. Koukoulitsa, T. Mavromoustakos, *Mol. Divers.* 14 (2) (2010) 257–276.
- [8] R. Galeazzi, *Curr. Comput. Aid Drug Design* 5 (2009) 225–240.
- [9] A. Makriyannis, X. Tian, J. Guo, *Prostagland. Lipid Mediat.* 77 (2005) 210–218.
- [10] R.P. Mason, D.G. Rhodes, L.G. Herbetto, *J. Med. Chem.* 34 (1991) 869–877.
- [11] D.F. Sargent, R. Schwyzer, *Proc. Natl. Acad. Sci. USA* 83 (1986) 5774–5778.
- [12] T. Kimura, *Biochemistry* 45 (2006) 15601–15609.
- [13] T. Kimura, E. Okamura, N. Matubayasi, K. Asami, M. Nakahara, *Biophys. J.* 87 (2004) 375–385.
- [14] T. Mavromoustakos, D.P. Yang, A. Charalambous, L.G. Herbetto, A. Makriyannis, *Biochim. Biophys. Acta Biomembr.* 1024 (1990) 336–344.
- [15] D.P. Yang, T. Mavromoustakos, K. Beshah, A. Makriyannis, *Biochim. Biophys. Acta Biomembr.* 1103 (1992) 25–36.
- [16] T. Mavromoustakos, D.P. Yang, A. Makriyannis, *Biochim. Biophys. Acta Biomembr.* 1237 (1995) 183–188.
- [17] T. Mavromoustakos, E. Theodoropoulou, D. Papahatjis, T. Kourouli, D.P. Yang, M. Trumbore, A. Makriyannis, *Biochim. Biophys. Acta Biomembr.* 1281 (2) (1996) 235–244.
- [18] T. Kimura, K. Cheng, K.C. Rice, K. Gawrisch, *Biophys. J.* 96 (2009) 4916–4924.
- [19] Sybyl Molecular Modeling Software. Tripos International, 1699 South Hanley Rd., St. Louis, Missouri, 63144, USA.
- [20] B.R. Brooks, R.E. Bruccoleri, B.D. Olafson, D.J. States, S. Swaminathan, M.M. Karplus, *J. Comput. Chem.* 4 (1983) 187–217.
- [21] G. Klebe, U. Abraham, T. Mietzer, *J. Med. Chem.* 37 (1994) 4130–4146.
- [22] M. Rarey, B. Kramer, T. Lengauer, G. Klebe, *J. Mol. Biol.* 261 (1996) 470–489.
- [23] T. Tuccinardi, P.L. Ferrarini, C. Manera, G. Ortore, G. Saccomanni, A. Martinelli, *J. Med. Chem.* 49 (2006) 984–994.
- [24] O.M.H. Salo, M. Lahtela-Kakkonen, J. Gynther, T. Jarvinen, A. Poso, *J. Med. Chem.* 47 (2004) 3048–3057.
- [25] J.Y. Shim, W.J. Welsh, A.C. Howlett, *Biopolymers* 71 (2003) 169–189.
- [26] D. van Der Spoel, E. Lindahl, B. Hess, G. Groenhof, A.E. Mark, H.J. Berendsen, *J. Comput. Chem.* 26 (2005) 1701–1717.
- [27] http://davapc1.bioch.dundee.ac.uk/cgi-bin/prodrg_beta.
- [28] <http://www.apmaths.uwo.ca/~mkarttu/downloads.shtml>.
- [29] H.J.C. Berendsen, J.P.M. Postma, W.F. van Gunsteren, A. DiNola, J.R. Haak, *J. Chem. Phys.* 81 (1984) 3684–3690.
- [30] U. Essmann, L. Perera, M.L. Berkowitz, T. Darden, H. Lee, L.G. Pedersen, *J. Chem. Phys.* 103 (1995) 8577–8593.
- [31] B. Hess, H. Bekker, H.J.C. Berendsen, J.G.E.M. Fraaije, *J. Comput. Chem.* 18 (1997) 1463–1472.
- [32] H. Wang, R.A. Duffy, G.C. Boykow, S. Chackalamannil, V.S. Madison, *J. Med. Chem.* 51 (2008) 2439–2446.
- [33] A.R. Leach, V.J. Gillet, R.A. Lewis, R. Taylor, *J. Med. Chem.* 53 (2010) 539–558.
- [34] S.P. Nikas, S.O. Alapafuja, I. Papanastasiou, C.A. Paronis, V.G. Shukla, D.P. Papahatjis, A.L. Bowman, A. Halikhedkar, X. Han, A. Makriyannis, *J. Med. Chem.* 53 (2010) 6996–7010.
- [35] D.P. Papahatjis, V. Kourouli, A. Abagji, A. Goutopoulos, A. Makriyannis, *J. Med. Chem.* 41 (1998) 1195–1200.
- [36] S. Durdagi, A. Kapou, T. Kourouli, T. Andreou, S.P. Nikas, V.R. Nahmias, et al., *J. Med. Chem.* 50 (2007) 2875–2885.